Molecular Orientation and Film Morphology of Pentacene on Native Silicon Oxide Surface

S. D. Wang, X. Dong, C. S. Lee, and S. T. Lee*

Center of Super-Diamond and Advanced Films (COSDAF) and Department of Physics and Materials Science, City University of Hong Kong, Hong Kong SAR, China

Received: August 4, 2004; In Final Form: April 11, 2005

The growth morphology and mechanism of pentacene films on native Si oxide surface have been studied by using high-resolution electron energy loss spectroscopy (HREELS), X-ray diffraction (XRD), and atomic force microscopy (AFM). Despite the good agreement between our own and the reported XRD results, the previous XRD interpretation that the pentacene molecules are tilt-standing on the substrate cannot explain our HREELS data. The HREELS results show that a substantial portion of the first two layers of pentacene molecules are tilted-standing or randomly oriented, whereas the upper-layer molecules are mostly lying flat to the substrate. AFM reveals that the first two layers of molecules form a flat and smooth surface, but the upper layers show a rough terrace structure with a mean-square roughness equal to the average thickness (without counting the first two layers). This relationship is explained by a theoretical model which assumes the pentacene molecules to remain on a particular molecule layer after arrival. The observed film growth morphology may have significant implication on the performance of electronic devices based on pentacene thin films. A plausible explanation was proposed for the discrepancy between the HREELS-indicated and the XRD-derived molecular orientations.

I. Introduction

Organic thin film transistors (OTFTs) have recently emerged as promising candidates in switching devices for active-matrix flat panel displays and as components in organic sensors, organic smart cards, etc.[1−5] Performance of OTFTs have been drastically improved in the past few years. Pentacene-based devices are shown to have performance comparable to that of hydrogenated amorphous silicon (a-Si:H).[6,7] It is well-known that carrier transport in organic films depends strongly on the extent of π-bond overlap between neighboring molecules. Thus the level of structural order and packing fashion of molecules can considerably influence the carrier mobility in the films. Numerous structural and morphological studies on vacuum-deposited pentacene thin films on Si oxide surfaces have been reported,[8−12] revealing two common phases of pentacene: the thermodynamically stable bulk-like phase and the metastable but kinetically favored thin-film phase. The crystalline structure of the bulk phase of pentacene is triclinic with two molecules in a unit cell, in which a slight deviation from monoclinic symmetry results in the close packing of molecules in the lattice.[13] According to X-ray diffraction (XRD), the thin-film phase is regarded as being similar to the bulk, having an elongated (001) plane spacing.[8,10] Hence the molecules in the thin-film phase are supposed to be tilted-standing with a herringbone arrangement within the (00*k*) planes. Here, we report a study on the molecular orientation and the film morphology of pentacene on native Si oxide surface. Our XRD and atomic force microscopy (AFM) results are in good agreement with the previous reports, whereas our high-resolution electron energy loss spectroscopy (HREELS) results reveal a flat-lying molecular orientation that is at variance with the prevalent view for the vacuum-deposited pentacene on Si oxide surface.

* Corresponding author. E-mail: apannale@cityu.edu.hk, Fax: 852−2784−4696.

II. Experimental Details

Pentacene (Arcos Organics, 98%) films were carefully prepared by thermal evaporation in ultrahigh vacuum (UHV). The base pressure in the deposition chamber and the working pressure during deposition were about 8×10^{-10} and 5×10^{-9} Torr, respectively. The deposition rate of pentacene was maintained at 1 nm per minute, and the substrate was at room temperature. The mean thickness of the deposited films was monitored by a quartz microbalance. Si substrates were chosen because the native Si oxide surface is similar to the oxide layer thermally grown on Si, which is widely used as the dielectric layer in OTFTs. HREELS measurements were performed with an LK Technologies model 3000 HREELS spectrometer, in which the base pressure was lower than 2×10^{-10} Torr. The spectra were collected in a specular geometry with an incident and exit angle of 62° measured from the surface normal. The primary electron energy was 6.0 eV, and the energy resolution was set at 5 meV. XRD spectra were measured in air with a Philips X'Pert-MRD (Cu Kα, 40 kV, 40 mA). Atomic force microscopy (AFM) images were recorded in the tapping mode in air with a Digital Instruments NanoScope IIIa probe microscope system.

III. Results and Discussions

Figure 1 shows the HREELS spectra of pentacene thin films on native Si oxide as a function of film thickness. The bottom spectrum (spectrum i) represents the vibrational spectrum of the substrate surface, in which the dominant loss bands at 56, 100, and 146 meV are related to the Si−O vibrational modes. The broadness of the loss bands originates from the amorphous nature of the native Si oxide layer.[14] After deposition of 0.7 nm pentacene, a representative loss peak d at 380 meV emerges in the HREELS spectrum (spectrum ii). According to its loss energy, the emerging loss peak can be assigned to the C−H stretch mode of aromatic compounds.[14,15] Three other peaks

10.1021/jp046490p CCC: $30.25
Published on Web 04/21/2005

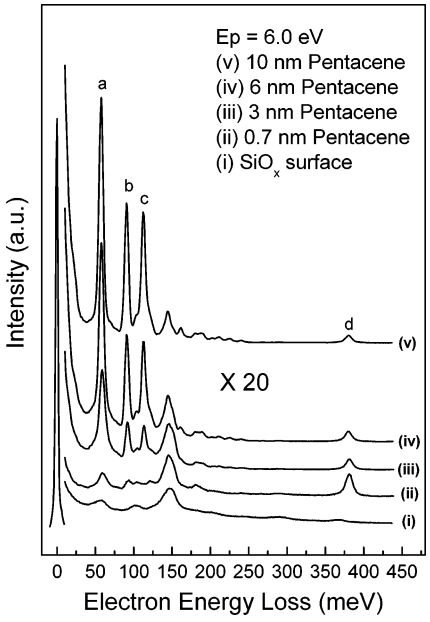

Figure 1. HREELS spectra of pentacene deposited on native Si oxide surface as a function of film thickness. "(ii)−(v)" represent the respective samples of different thickness, and "a−d" denote the dominant loss peaks of pentacene.

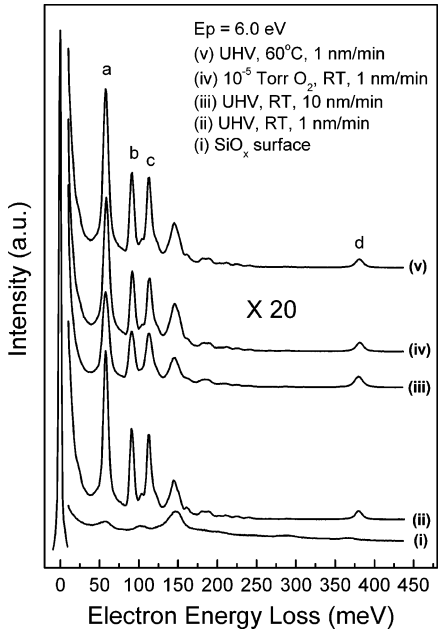

Figure 2. Comparison of HREELS spectra of 6 nm pentacene films prepared under different deposition conditions.

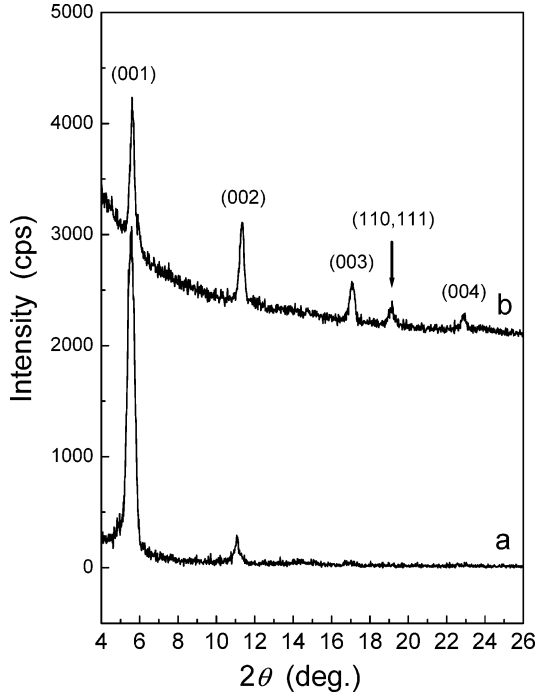

Figure 3. XRD spectra of a 5 nm pentacene film (a) and a 20 nm pentacene film (b).

grow up quickly in the thicker films, (spectra iii−v). Peak a at 58 meV is associated with the out-of-plane ring bend mode, while peaks b and c correspond to the out-of-plane C−H bend modes.[14,15] Assignments of the loss peaks are in good agreement with the infrared data.[16]

The HREELS spectra in Figure 1 show that the ratios of the intensity of the out-of-plane bend modes (peaks a, b, and c) to that of the in-plane mode (peak d) increase dramatically with increasing film thickness. In the thicker films (spectra iii−v), the intensities of the out-of-plane modes are much stronger than that of the in-plane mode. As HREELS can provide insightful information on the orientation of planar molecules in thin films,[17] it is used here for similar analysis. For pentacene molecules, the polarization of the C−H stretch mode is in the molecular plane, whereas that of the out-of-plane bend modes is perpendicular to the molecular plane. Since our HREELS results are collected in the specular direction, the vibrational modes perpendicular to the surface are strongly excited by dipole scattering, and those parallel to the surface are only weakly excited due to screening of image charges.[14] Therefore, the large and rapid increase of the intensity of the out-of-plane bend modes relative to that of the in-plane stretch mode implies that the orientation of pentacene molecules in the first few monolayers is different from that in the upper layers. In the initial growth stage, pentacene molecules appear to nucleate on the substrate with a tilted-standing or random orientation, so that the in-plane stretch mode (peak d) is more intense than the out-of-plane bend modes (peaks a, b, and c). In spectrum ii, the intensity of the out-of-plane bend mode (peak a) is comparable to that of the in-plane stretch mode (peak d), and the vibrational features of the substrate are still visible. With increasing pentacene thickness, the out-of-plane bend modes grow quickly in intensity and become the dominant peaks, as shown in spectra iii−v. The results suggest that most of the pentacene molecules in the upper layers change to a flat-lying orientation with their molecular plane parallel to the substrate surface. In recent reports, pentacene molecules were also found to adsorb in a similar flat-lying geometry, though in different crystalline structures, on Au (111) and on Si (100).[18,19]

Figure 2 shows a comparison of the HREELS spectra of the 6 nm pentacene films prepared under different deposition conditions. Upon changing the deposition rate, the base pressure, and the substrate temperature (Figure 2 iii, iv, and v, respectively), the spectra do not show much difference. The high ratio of the intensity of the out-of-plane bend modes to that of the in-plane mode is still obvious in the spectra, indicating that the flat-lying molecular orientation of pentacene in the upper layers is independent of the deposition parameters.

XRD spectra of the pentacene thin films on native Si oxide are shown in Figure 3. Only two peaks are observed in the spectrum of the 5 nm thick pentacene film (Figure 3a), versus five diffraction peaks in the 20 nm thick film (Figure 3b). The observation of diffraction peaks of higher Miller-index might

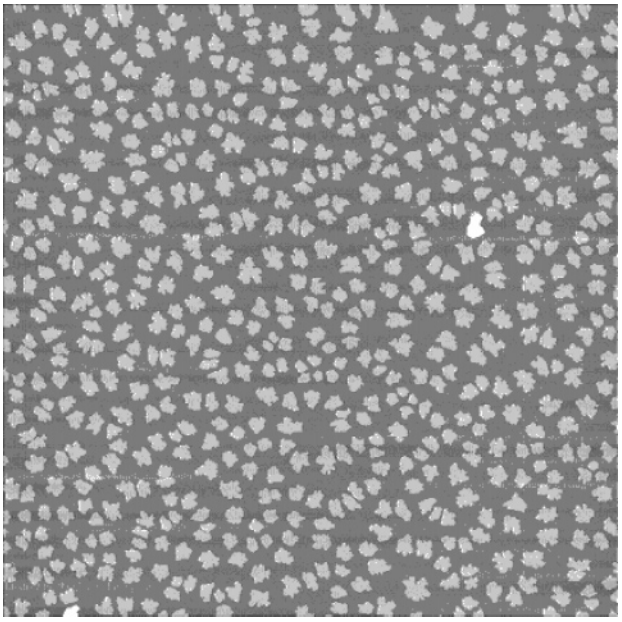

Figure 4. 10 μm × 10 μm AFM image of the 1 nm pentacene film.

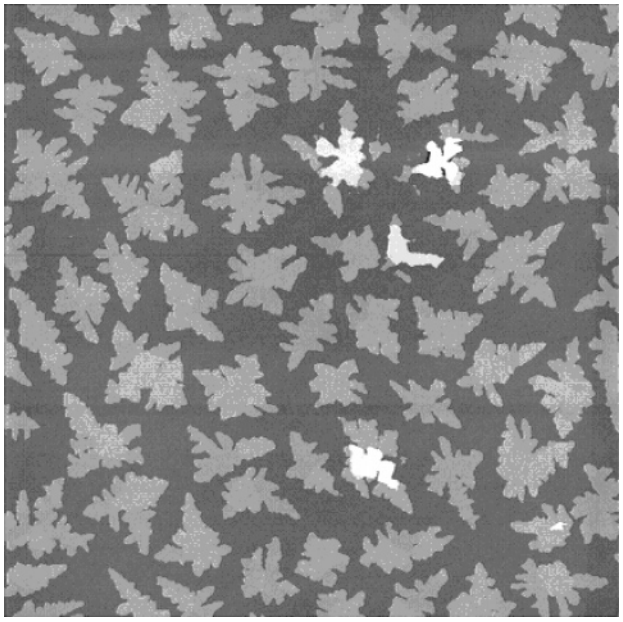

Figure 5. 10 μm × 10 μm AFM image of the 3 nm pentacene film.

be due to increased sample thickness and/or higher proportion of molecules in the corresponding molecular orientations. The angle positions of the four main peaks at 5.7, 11.4, 17.1, and 22.8 degrees are consistent with the reported values.[6−9] An extra diffraction feature is observed at about 19°, which has also been observed in the pentacene thin films deposited on octadecyltrichlorosilane-pretreated Si oxide surfaces.[10] The main peaks were previously interpreted as the (001), (002), (003), and (004) peaks of the well-known thin-film phase.[6−9] All XRD results led to the conclusion that pentacene molecules are in a tilted-standing orientation on the substrate and have a (001) interplanar spacing of about 1.55 nm. However, the XRD conclusion is at variance with the present HREELS results, which suggest most of the pentacene molecules in the upper layers are parallel to the substrate. The discrepancy will be discussed later.

Morphology of the pentacene films on native Si oxide surface was further analyzed using AFM. Figure 4 is a 10 μm × 10 μm AFM image of a 1 nm thick pentacene film, showing that submicron-sized islands are distributed on the substrate. With increasing pentacene thickness, the islands keep the same height of about 2.0 nm, but grow laterally from the island edges. After the formation of a continuous first layer, micron-sized islands in the second layer emerge with a height of about 1.6 nm. The 10 μm × 10 μm AFM image of a 3 nm thick pentacene film, depicted in Figure 5, shows the distribution of the islands in the second layer. These islands also grow laterally from the edges and finally form the almost continuous second layer, which is illustrated by the 10 μm × 10 μm AFM image of about 4 nm pentacene in Figure 6. The RMS roughness of the substrate surface and that of the first two continuous layers are about 0.42 and 0.18 nm, respectively. It shows that the sample surface becomes smoother with further deposition of pentacene.

The growth of pentacene in the upper layers (after the first two layers) changes in a distinctively different way. The 4 μm × 4 μm AFM image of 6 nm pentacene (Figure 7) shows a terrace morphology on the surface. After further deposition of pentacene, the terrace structure of the upper layers becomes more evident, as clearly shown in the 4 μm × 4 μm AFM image of 12 nm pentacene (Figure 8). The morphology of pentacene is typical on Si oxide substrates, as reported by several other groups.[20,21] The AFM results also indicate that the height of

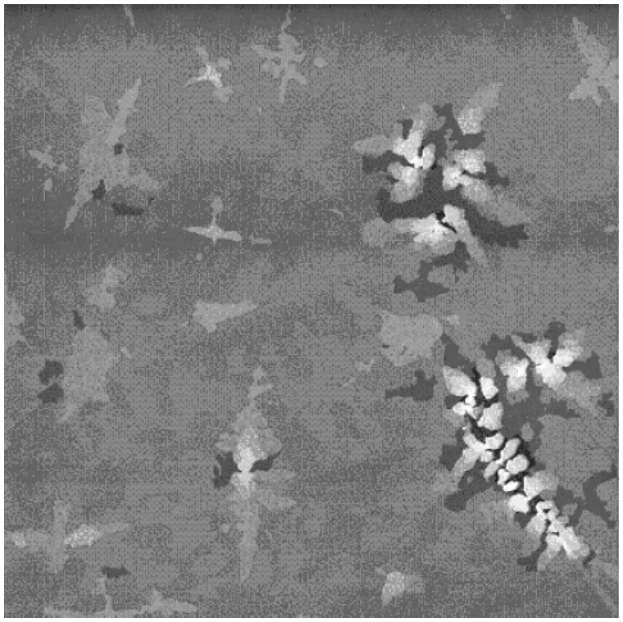

Figure 6. 10 μm × 10 μm AFM image of the 4 nm pentacene film.

each layer in the terraces is close to that of the others, around 1.6 nm. This value is the same as the height of the continuous second layer, and is approximately in agreement with the periodic distance of 1.55 nm as deduced from the XRD data.

A schematic description of the cross section of the pentacene films is shown in Figure 9. To interpret the terrace formation in the upper layers, the following assumption is used. When a pentacene molecule is deposited on an upper layer, its movement is restricted to this particular layer alone. In other words, the molecule cannot jump to the upper or lower layers after its arrival. According to this assumption, the following differential equation can be obtained:

$$\frac{d}{dt}C_i = R(C_{i-1} - C_i)\ (i > 2)$$

where C_i is the coverage of the ith layer, R is the deposition rate, and t represents time. Considering the initial conditions of $t = 0$, $C_2 = 1$ and $C_i = 0$ ($i > 2$), and integrating

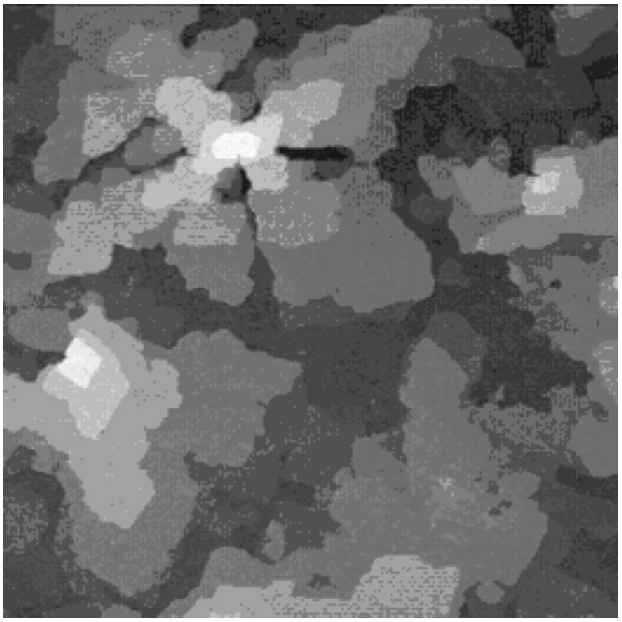

Figure 7. 4 μm × 4 μm AFM image of the 6 nm pentacene film.

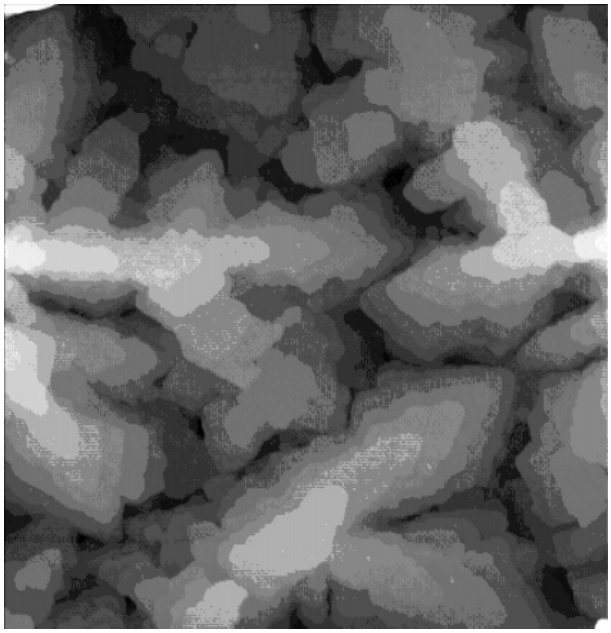

Figure 8. 4 μm × 4 μm AFM image of the 12 nm pentacene film.

the differential equation gives:

$$\Delta C_{i-1} = C_{i-1} - C_i = \frac{(Rt)^{i-3}}{(i-3)!} e^{-Rt} \quad (i > 2)$$

where ΔC_i is the uncovered percentage of the ith layer, and Rt expresses the product of the deposition rate and time, which corresponds to the mean thickness T. The equation can be rewritten in terms of T as

$$\Delta C_{i-1} = \frac{T^{i-3}}{(i-3)!} e^{-T} \quad (i > 2)$$

This equation is in fact exactly an expression of the Poisson distribution, which defines the theoretical relationship between the mean thickness of the film and the uncovered percentage of the upper layers. In a Poisson distribution, the mean-square variance should be equal to the average value. In the present case, the average value is the mean thickness T, and the square of the RMS roughness in the AFM images corresponds to the mean-square variance; that is T should be equal to the mean-square roughness. Figure 10 shows a plot of the mean-square roughness as a function of the mean thickness using the data obtained from the AFM study. It is clear that the mean-square roughness shows a linear relationship with the mean thickness, and the slope of the fitted straight line is close to 1. Moreover, the x intercept in Figure 10 appears at around 3.7 nm, which is exactly the total thickness of the first two layers. The experimental results agree very well with the theoretically derived expectation, implying that the assumption of the lack of the interlayer diffusion is tenable.

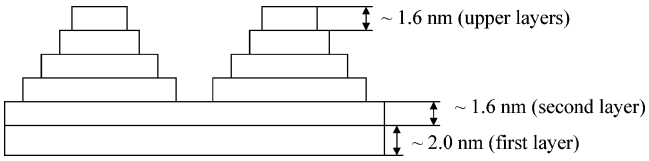

Figure 9. Schematic description of the cross section of the pentacene film.

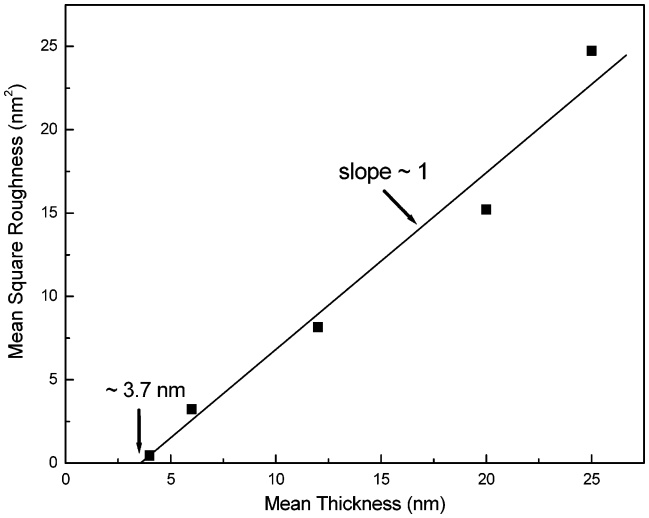

Figure 10. Mean-square roughness as a function of mean thickness of the pentacene films.

From the morphological results, we propose the following picture of the film growth process. In the initial stage of growth, the pentacene molecules nucleate to form the two-dimensional (2D) islands (Figure 4) at the substrate defects,[22] and these islands grow laterally from the edges and ultimately form a complete layer. After the full coverage of the first two layers (Figure 6), the layer-by-layer growth abruptly changes to the three-dimensional (3D) island growth, and eventually a terrace structure forms on the completed layers (Figure 8). The layer plus island growth process thus follows the Stranski−Krastanov (S−K) growth mode, which is an intermediate mode between the Frank-van der Merwe (F-vdM) layer-by-layer growth mode and the Volmer−Weber (V−M) island growth mode.[23,24] S−K growth commonly occurs in strain systems,[25,26] in which strain induced by lattice mismatch is relaxed by forming thick islands with interfacial misfit dislocations. However, the transition from layer-by-layer to island growth in the pentacene case is more likely due to the change of the adsorption energy on the exposed surfaces. In the initial deposition, the adsorption energy of pentacene on the substrate is comparatively high, so that the pentacene molecules are more strongly bound to the substrate than to each other, thus resulting in the formation of the first complete layer. The larger size of the 2D nuclei on the second

layer (Figure 5) suggests the lower adsorption energy of pentacene on the first adsorbed layer, though the edge growth is still favored. The transition of the growth mode may be attributable to the change of the molecular orientation during the growth as revealed by HREELS, which can lead to a further decrease of the adsorption energy over a critical value on the second adsorbed layer. In the subsequent deposition pentacene molecules are more strongly bound to each other than to the adsorbed layers, and thus island growth becomes favored in the upper layers. Furthermore, the lack of the interlayer diffusion mentioned above, probably due to a high diffusion barrier at the edges of the upper layers, may further enhance the island formation.

The discontinuous nature of the upper layers may lead to an extremely poor conductivity, and possibly more undesirable carrier trapping. Moreover, the flat-lying molecules, possessing a low degree of π-overlap in the horizontal direction, are expected to result in a low mobility for the carriers transporting in the upper layers. Hence, in the OTFTs using pentacene as the active layer, the first few monolayers of pentacene not only play the important role of carrier accumulation, but also act as the carrier transporting layer. Due to the important effect of organic layers on eventual electronic devices, the present work points to the need for more work, in particular on the film structure and growth morphology and how they influence the electronic properties.

Finally, we discuss the discrepancy between the conclusions drawn from the HREELS and the XRD-derived results. According to the 1.55 nm periodic distance from XRD and the identical 1.6 nm layer height from AFM, one may reasonably believe that the molecular orientation of pentacene is tilted-standing. However, the present HREELS results indicate that most of the pentacene molecules are flat-lying in the upper layers. A plausible explanation for the apparent discrepancy is to assume the presence of a new phase in which the molecules are parallel to the substrate with a lattice spacing of 1.55 nm in the normal direction. We note that if the new phase were formed only by simple stacking of flat-lying pentacene molecules, XRD should have given patterns with larger angles corresponding to a much smaller periodic distance. However, the proposed assumption cannot be excluded because the periodic distance may be reduplicated by taking into account the displacements during the stacking and the small angle titling of the molecular planes. Unfortunately, the present experimental data do not provide supporting evidence for the assumption; thus more experiments are needed.

IV. Summary

Structural and morphological studies of pentacene grown on native Si oxide surface were carried out. The HREELS results indicate that the molecular orientation of pentacene in the initial few monolayers is different from that in the upper layers. Most of the pentacene molecules in the upper layers adopt a flat-lying orientation with their molecular plane parallel to the substrate surface, whereas the molecules in the first several monolayers behave differently. The present XRD results are in good agreement with the previous XRD reports, showing the tilted-standing molecular orientation of pentacene, which is at variance with the flat-lying orientation deduced from our HREELS finding. We have attempted to explain the discrepancy, which remains unclear and requires further studies. AFM investigations reveal that the pentacene molecules in the first two layers form continuous films by edge growth, while the upper layers adopt a terrace structure.

Acknowledgment. This work was supported by the Central Allocation Scheme of the Research Grants Council of Hong Kong SAR (Projects No. CityU 2/02C), China.

References and Notes

(1) Wisnieff, R. *Nature* **1998**, *394*, 225.
(2) Horowitz, G. *Adv. Mater.* **1998**, *10*, 365.
(3) Crone, B.; Dodabalapur, A.; Gelperin, A.; Torsi, L.; Katz, H. E.; Lovinger, A. J.; Bao, Z. *Appl. Phys. Lett.* **2001**, *78*, 2229.
(4) Dimitrakopoulos, C. D.; Malenfant, P. R. L. *Adv. Mater.* **2002**, *14*, 99.
(5) Halik, M.; Klauk, H.; Zschieschang, U.; Schmid, G.; Ponomarenko, S.; Kirchmeyer, S.; Weber, W. *Adv. Mater.* **2003**, *15*, 917.
(6) Lin, Y. Y.; Gundlach, D. J.; Nelson, S.; Jackson, T. N. *IEEE Electron Device Lett.* **1997**, *18*, 606.
(7) Dimitrakopoulos, C. D.; Purushothaman, S.; Kymissis, J.; Callegari, A.; Shaw, J. M. *Science* **1999**, *283*, 822.
(8) Dimitrakopoulos, C. D.; Brown, A. R.; Pomp, A. *J. Appl. Phys.* **1996**, *80*, 2501.
(9) Venuti, E.; Valle, R. G. D.; Brillante, A.; Masino, M.; Girlando, A. *J. Am. Chem. Soc.* **2002**, *124*, 2128.
(10) Shtein, M.; Mapel, J.; Benziger, J. B.; Forrest, S. R. *Appl. Phys. Lett.* **2002**, *81*, 268.
(11) Casalis, L.; Danisman, M. F.; Nickel, B.; Bracco, G.; Toccoli, T.; Iannotta, S.; Scoles, G. *Phys. Rev. Lett.* **2003**, *90*, 206101.
(12) Kang, S. J.; Noh, M.; Park, D. S.; Kim, H. J.; Whang, C. N.; Chang, C. H. *J. Appl. Phys.* **2004**, *95*, 2293.
(13) Silinsh, E. A.; Capek, V. *Organic Molecular Crystals*; American Institute of Physics: New York, 1994.
(14) Ibach, H.; Mills, D. L. *Electron Energy Loss Spectroscopy and Surface Vibrations*; Academic Press: London, 1982.
(15) Ding, X. M.; Huang, L. M.; Lee, C. S.; Lee, S. T. *Phys. Rev. B* **1999**, *60*, 13291.
(16) Hudgins, D. M.; Sandford, S. A. *J. Phys. Chem. A* **1998**, *102*, 344.
(17) Wang, S. D.; Dong, X.; Lee, C. S.; Lee, S. T. *J. Phys. Chem. B* **2004**, *108*, 1529.
(18) Meyer zu Heringdorf, F. J.; Reuter, M. C.; Tromp, R. M. *Nature* **2001**, *412*, 517.
(19) Kang, J. H.; Zhu, X. Y. *Appl. Phys. Lett.* **2003**, *82*, 3248.
(20) Bouchoms, I. P. M.; Schoonveld, W. A.; Vrijmoeth, J.; Klapwijk, T. M. *Synth. Met.* **1999**, *104*, 175.
(21) Knipp, D.; Street, R. A.; Völkel, A.; Ho, J. *J. Appl. Phys.* **2003**, *93*, 347.
(22) Lukas, S.; Witte, G.; Wöll, Ch. *Phys. Rev. Lett.* **2002**, *88*, 28301.
(23) Bauer, E. *Z. Kristallogr.* **1958**, *110*, 372.
(24) Venables, J. A.; Spiller, G. D. T.; Hanbücken, M. *Rep. Prog. Phys.* **1984**, *47*, 399.
(25) Eaglesham, D. J.; Cerullo, M. *Phys. Rev. Lett.* **1990**, *64*, 1943.
(26) Shchukin, V. A.; Ledenstov, N. N.; Kopev, P. S.; Bimberg, D. *Phys. Rev. Lett.* **1995**, *75*, 2968.